Supporting Information (SI)

Sulfonylcalix[4]arene-based Al_4 clusters: three aluminum oxo clusters with different coordinated solvents for the CO_2 cycloaddition reaction

Xiao-Jie Liu, Long-Xue Guo, Wei Xu, Ya-Wen Wang, Yuan-Hang Tian, Li-Xing Zhao, Xiao-Yu Li*, Jin-Hua Li*, and Guo-Ming Wang

College of Chemistry and Chemical Engineering, Qingdao University, Shandong 266071, P. R. China

Email: xylichem@qdu.edu.cn; jinhuali1978@163.com

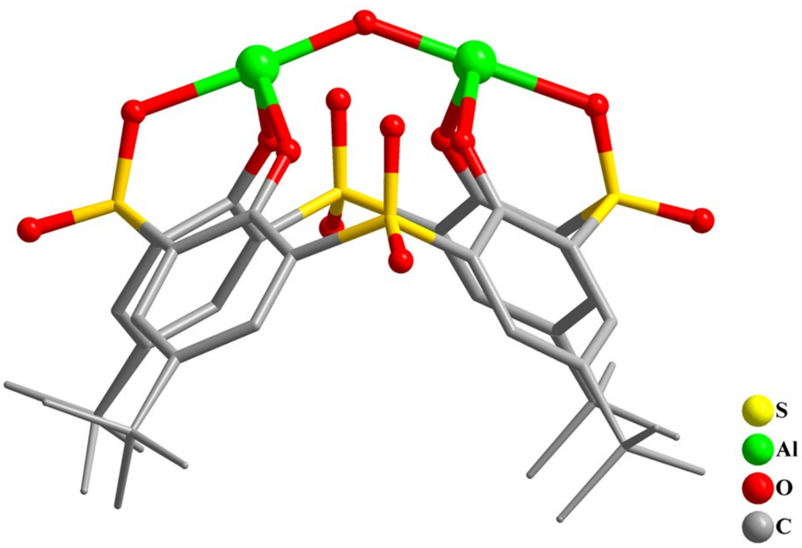

Fig. S1 The coordination modes of BTC4A-SO_2^{4-} ligand.

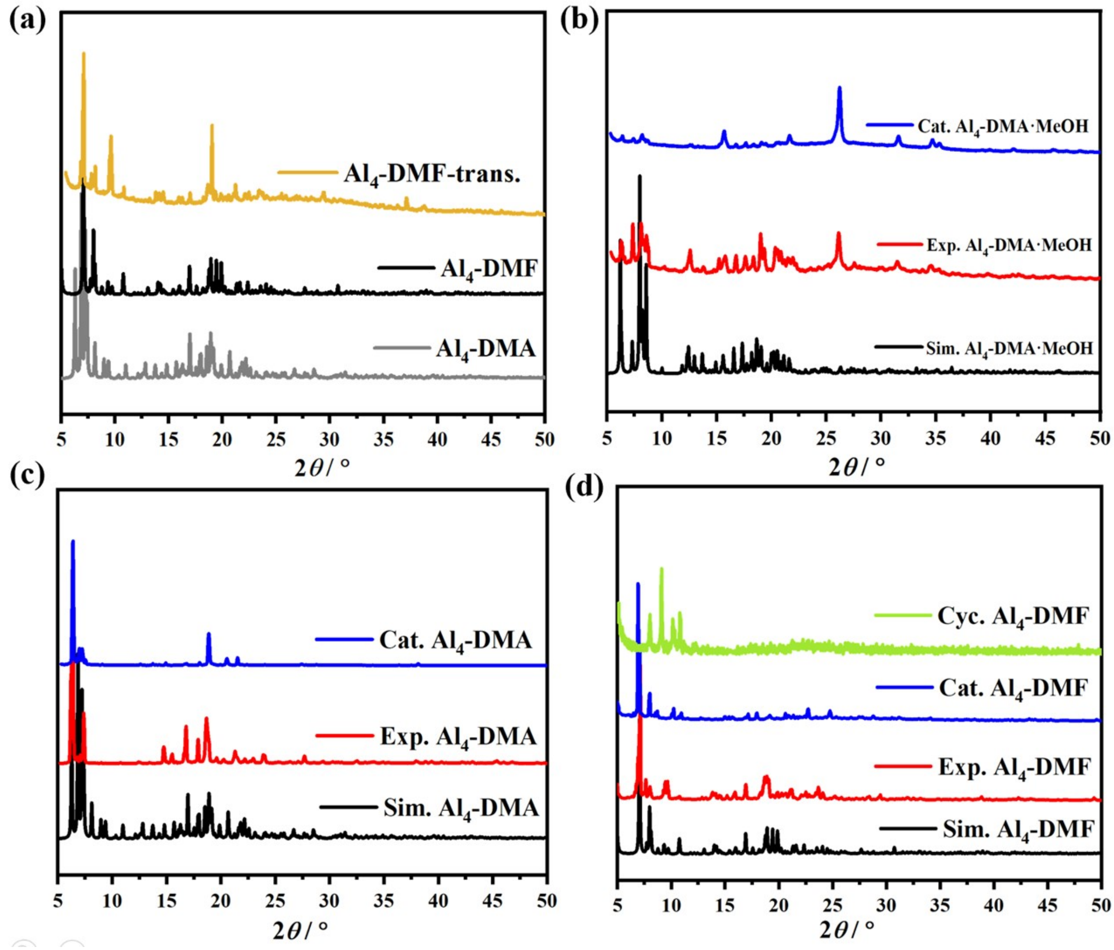

Fig. S2 The conversion powder from **Al_4-DMA** to **Al_4-DMF** (a), the simulated, experimental and catalyzed PXRD of **Al_4-DMA·MeOH** (b), **Al_4-DMA** (c), and simulated, experimental, catalyzed and cyclic PXRD of **Al_4-DMF** (d).

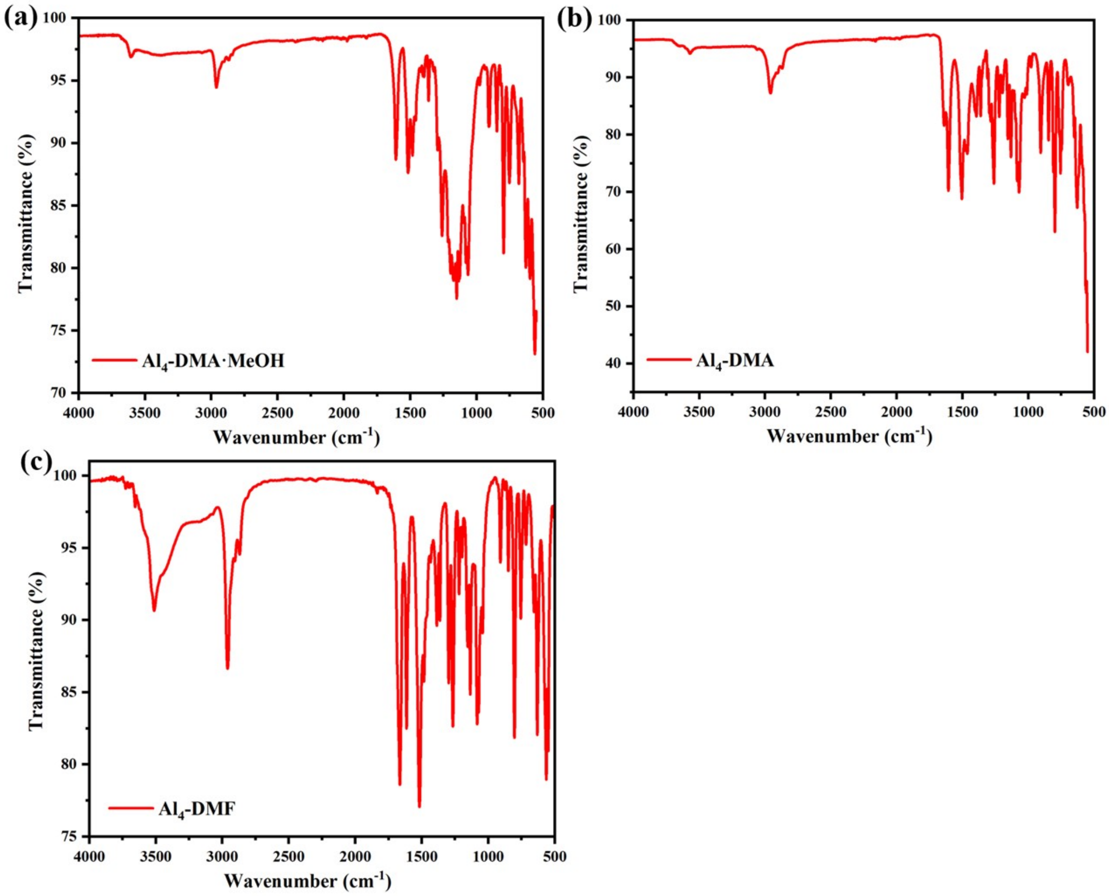

Fig. S3 The IR spectra of **Al_4-DMA·MeOH** (a), **Al_4-DMF** (b) and **Al_4-DMA** (c).

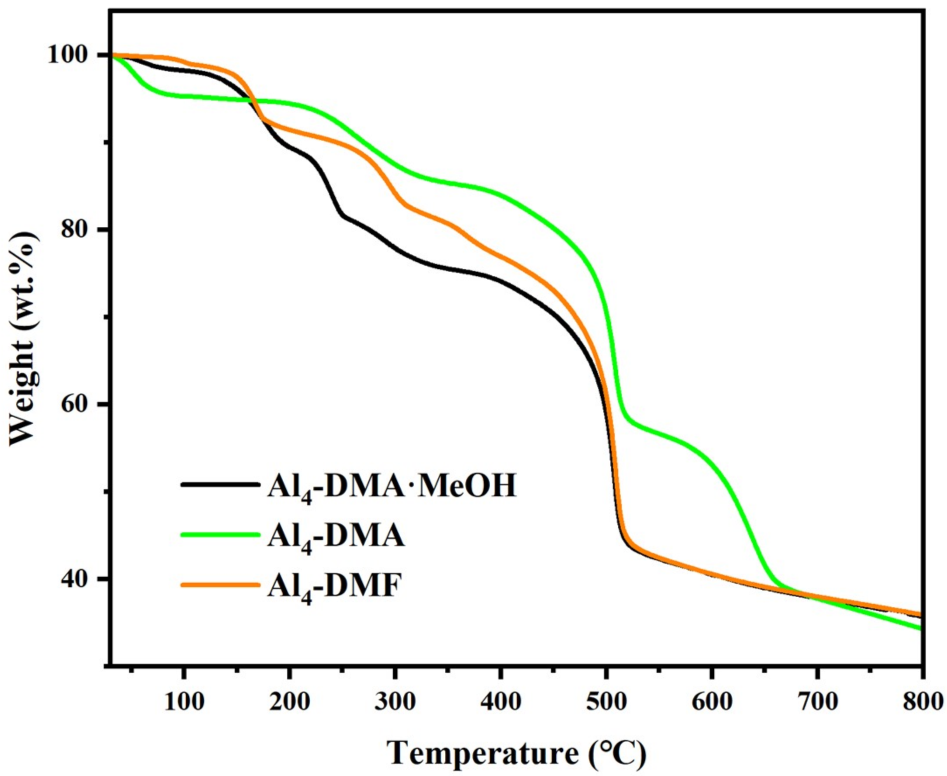

Fig. S4 The TGA of **Al_4-DMA·MeOH**, **Al_4-DMA** and **Al_4-DMF.**

Table S1. The formulas assignment of **Al_4-DMA·MeOH**, **Al_4-DMA** and **Al_4-DMF** in $CHCl_3$.

Species	Peak assignment	Exp.*m/z*	Sim.*m/z*
Al_4-DMA·MeOH			
1a	$[(Al)_4(OH)_3(BTC_4A\text{-}SO_2)_2(MeO)_2]^-$	1909.30	1909.31
1b	$[(Al)_4(OH)_3(BTC_4A\text{-}SO_2)_2(MeO)_2(MeOH)_1(H_2O)_1]^-$	1959.24	1959.35
1c	$[(Al)_4(OH)_3(BTC_4A\text{-}SO_2)_2(MeO)_2(MeOH)_1(H_2O)_2]^-$	1977.25	1977.36
1d	$[(Al)_4(OH)_3(BTC_4A\text{-}SO_2)_2(MeO)_2(MeOH)_2(H_2O)_1]^-$	1991.27	1991.38
1e	$[(Al)_4(OH)_3(BTC_4A\text{-}SO_2)_2(MeO)_2(DMA)_1(MeOH)_1(H_2O)_1]^-$	2047.30	2047.42
Al_4-DMA			
2a	$[(Al)_4(OH)_4(BTC_4A\text{-}SO_{2)2}(DMA)_3(H_2O)_7(Cl)_1]^-$	2288.55	2288.53
Al_4-DMF			
3a	$[(Al)_4(OH)_5(BTC_4A\text{-}SO_2)_2(H_2O)_1]^-$	1899.26	1899.29
3b	$[(Al)_4(OH)_5(BTC_4A\text{-}SO_2)_2(^n PrOH)_1]^-$	1941.25	1941.34
3c	$[(Al)_4(OH)_5(BTC_4A\text{-}SO_2)_2(^n PrOH)_1(H_2O)_1]^-$	1959.24	1959.35
3d	$[(Al)_4(OH)_5(BTC_4A\text{-}SO_2)_2(^n PrOH)_1(H_2O)_2]^-$	1977.25	1977.36
3e	$[(Al)_4(OH)_5(BTC_4A\text{-}SO_2)_2(DMF)_1(^n PrOH)_1(H_2O)_2]^-$	2051.31	2051.42

Table S2. The effect of temperature, pressure and time on cycloaddition of CO_2 catalyzed by **Al_4-DMF** was studied.

Entry	T [°C]	P [MPa]	Time [h]	Yield of **Al_4-DMF** (%)
1	80	0.1	4	83
2	80	0.5	4	99
3	80	1	4	99
4	80	2	4	99
5	70	0.5	4	85
6	60	0.5	4	77
7	80	0.5	3	62
8	80	0.5	4	99
9	80	0.5	5	99

Reaction conditions: epichlorohydrin (5.0 mmol), **Al_4-DMF** (0.01 mol%), $^{n}Bu_4NBr$ (3 mol%) solvent free.

Table S3. The effects of the amount of catalyst and cocatalyst and the synthesis material of **Al_4-DMF** cluster on the cycloaddition reaction of CO_2 catalyzed by **Al_4-DMF** were studied.

Entry	$^{n}Bu_4NBr$	**Al_4-DMF**	Yield of **Al_4-DMF** (%)
1	1 mol%	0.01 mol%	58
2	3 mol%	0.01 mol%	99
3	5 mol%	0.01 mol%	99
4	3 mol%	0	71
5	3 mol%	0.03 mol%	99
6	3 mol%	0.05 mol%	99
7	3 mol%	H_4BTC_4A-SO_2+$AlCl_3 \cdot 6H_2O$	78
8	3 mol%	DMA	73
9	3 mol%	DMF	72

Reaction conditions: epichlorohydrin (5.0 mmol), CO_2 (0.5 MPa), temperature (80 °C), time (4 h), solvent free.

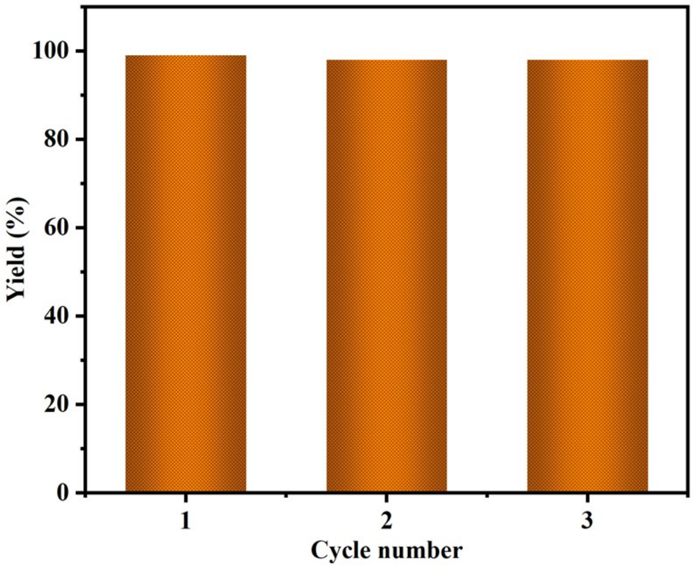

Fig. S5 Recyclability experiments for catalytic activities of **Al_4-DMF** in cycloaddition reaction.

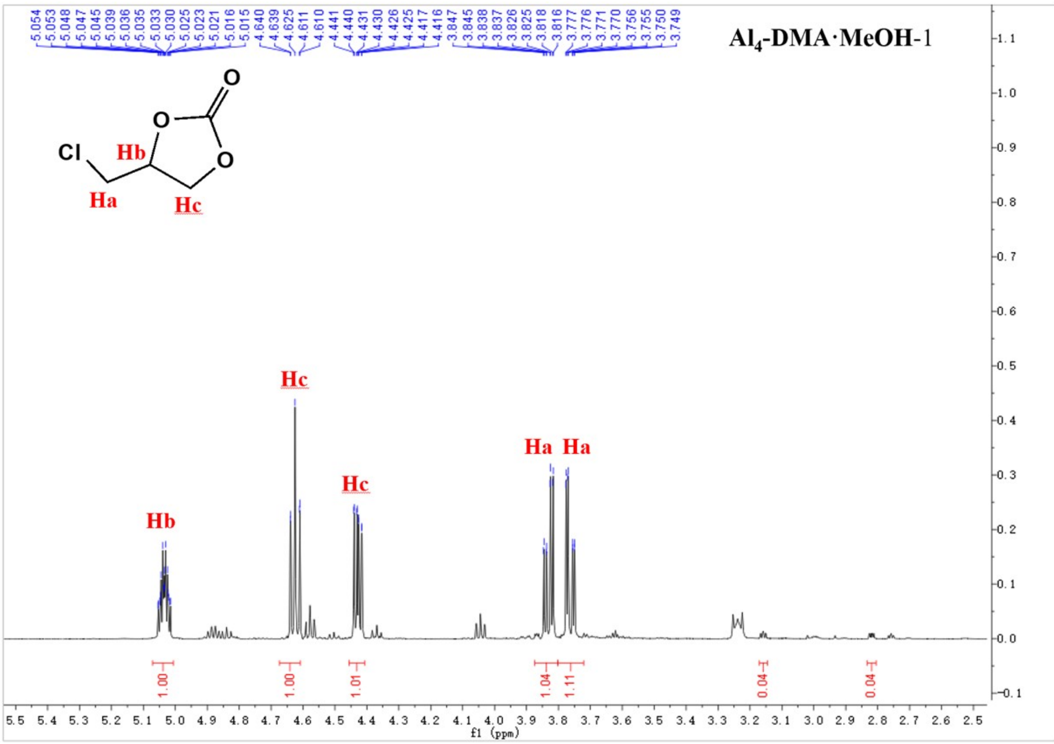

Fig. S6 [1]HNMR spectrum of **Al$_4$-DMA·MeOH**-1 catalyzed oxidation products of epichlorohydrin (400 MHz, $CDCl_3$, 298 K).

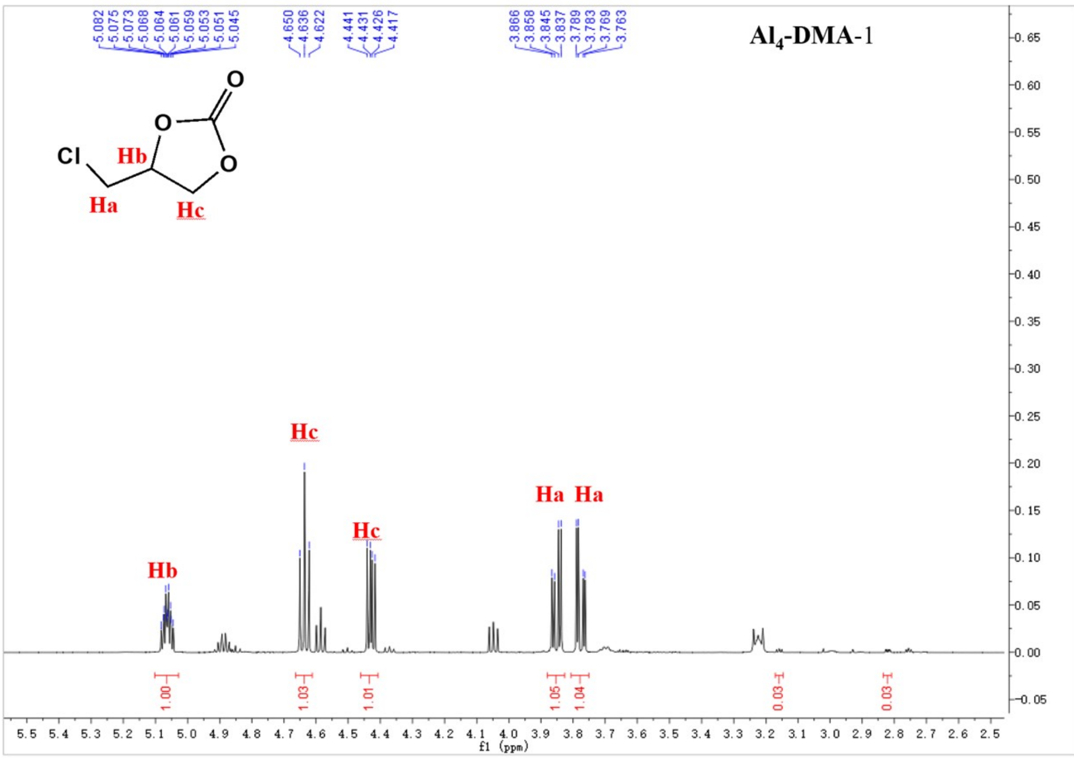

Fig. S7 [1]HNMR spectrum of **Al$_4$-DMA**-1 catalyzed oxidation products of epichlorohydrin (400 MHz, $CDCl_3$, 298 K).

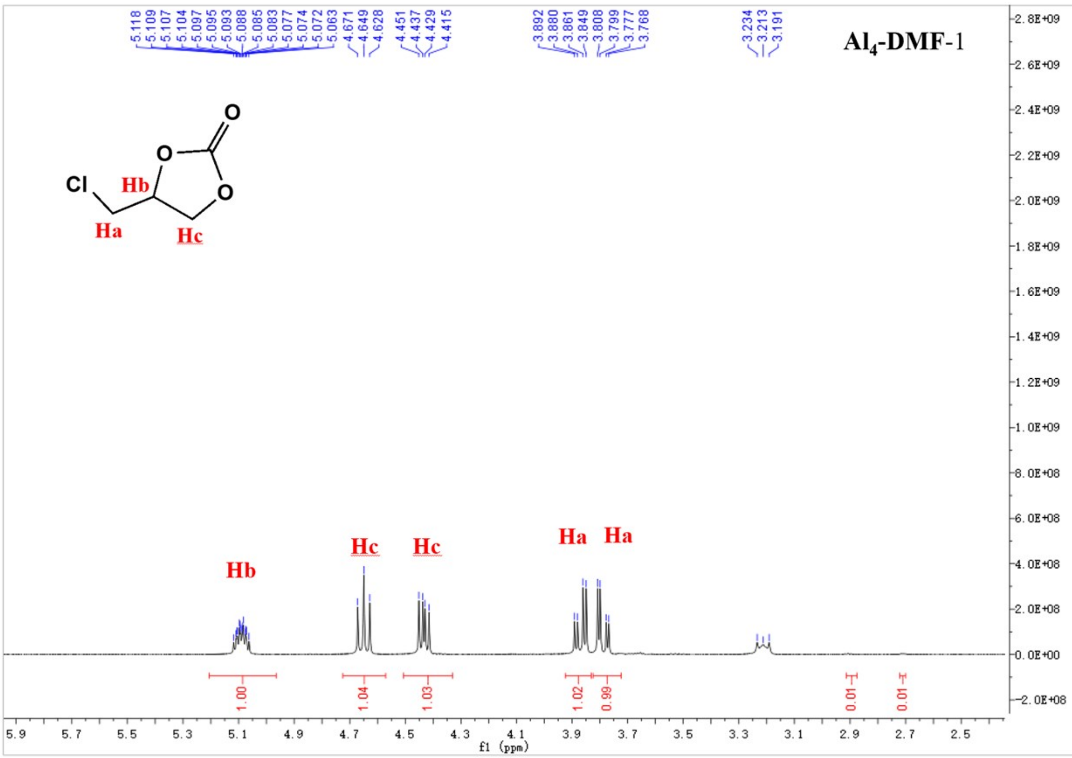

Fig. S8 [1]HNMR spectrum of **Al$_4$-DMF**-1 catalyzed oxidation products of epichlorohydrin (400 MHz, $CDCl_3$, 298 K).

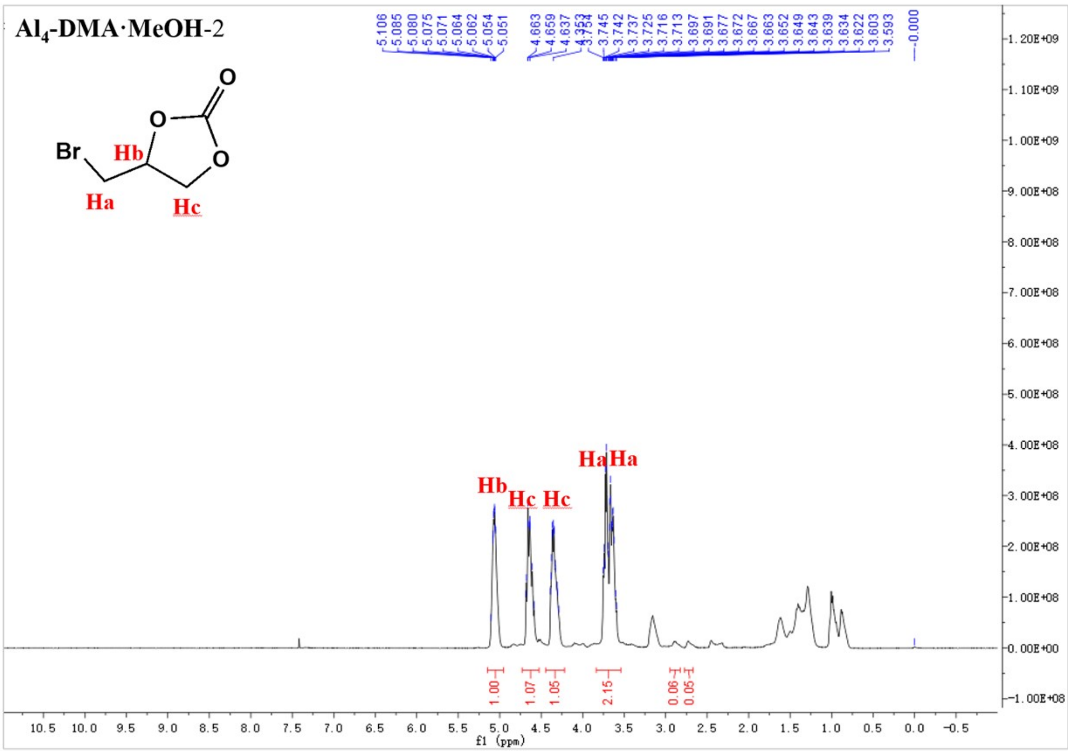

Fig. S9 [1]HNMR spectrum of **Al$_4$-DMF·MeOH**-2 catalyzed oxidation products of epoxybromopropane (400 MHz, $CDCl_3$, 298 K).

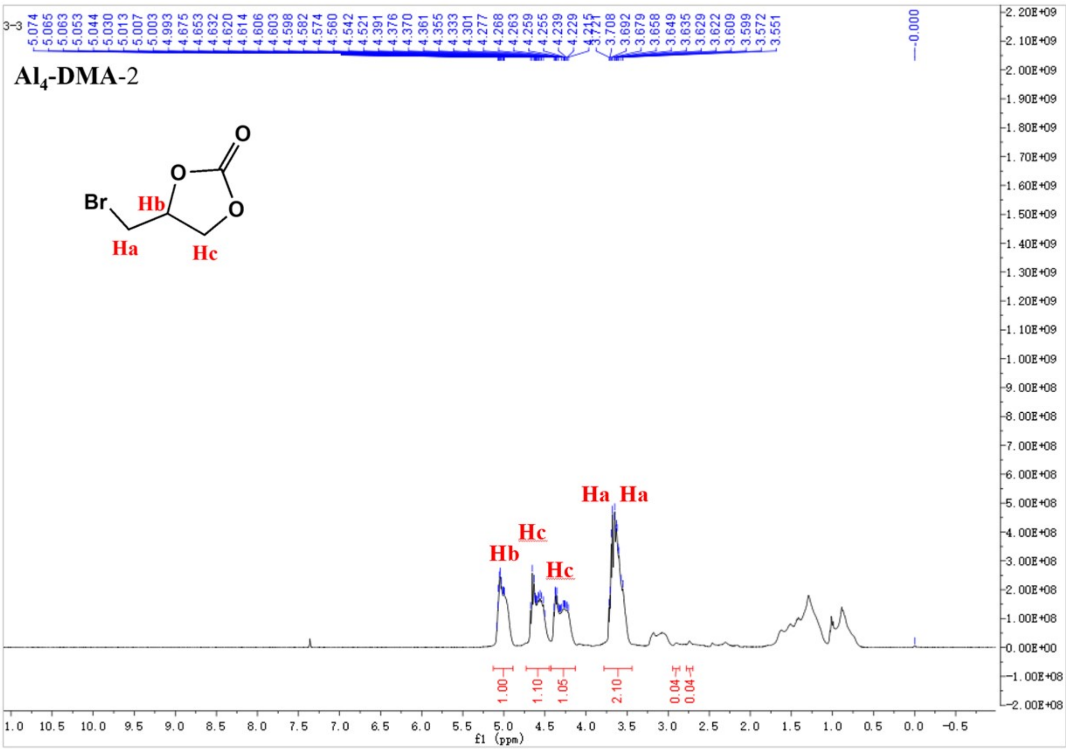

Fig. S10 [1]HNMR spectrum of **Al_4-DMA**-2 catalyzed oxidation products of epoxybromopropane (400 MHz, $CDCl_3$, 298 K).

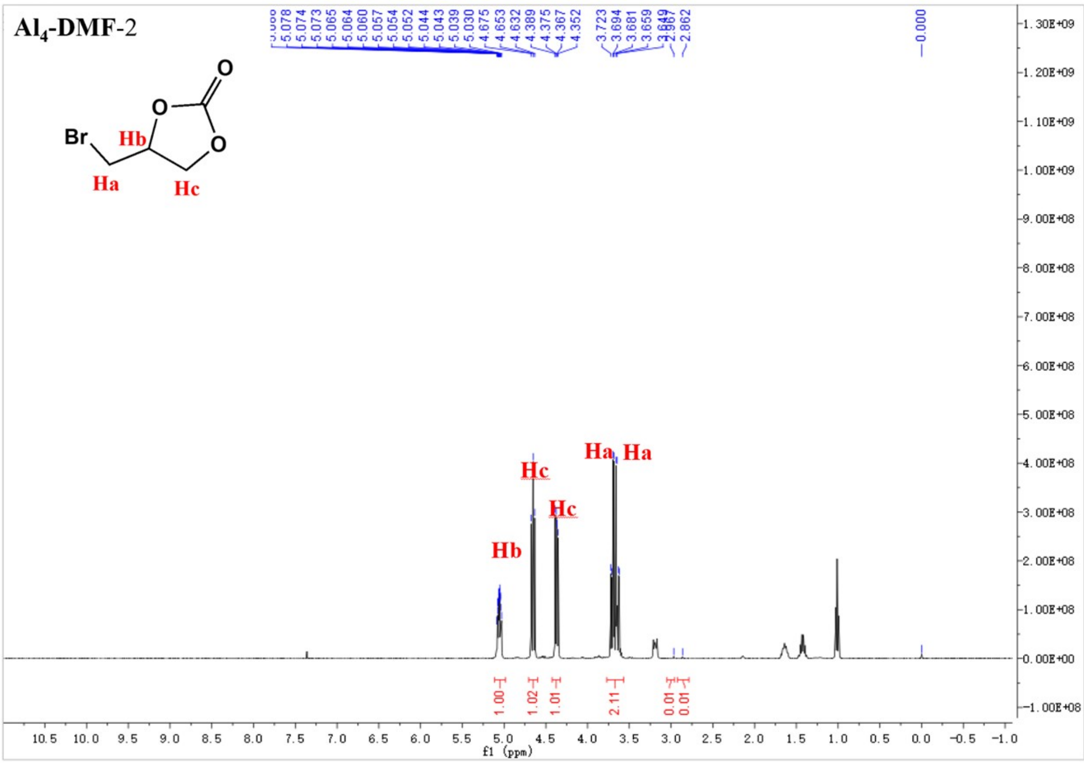

Fig. S11 [1]HNMR spectrum of **Al_4-DMF**-2 catalyzed oxidation products of epoxybromopropane (400 MHz, $CDCl_3$, 298 K).

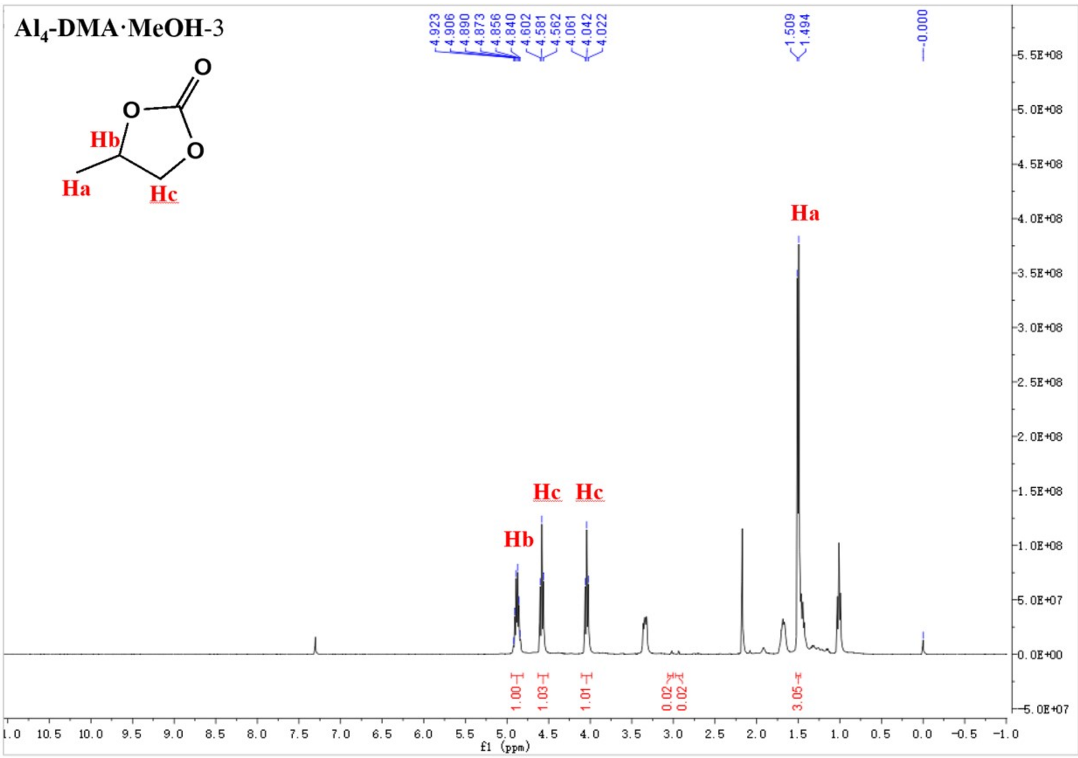

Fig. S12 ^{1}HNMR spectrum of **Al$_4$-DMA·MeOH**-3 catalyzed oxidation products of ethylene oxide (400 MHz, $CDCl_3$, 298 K).

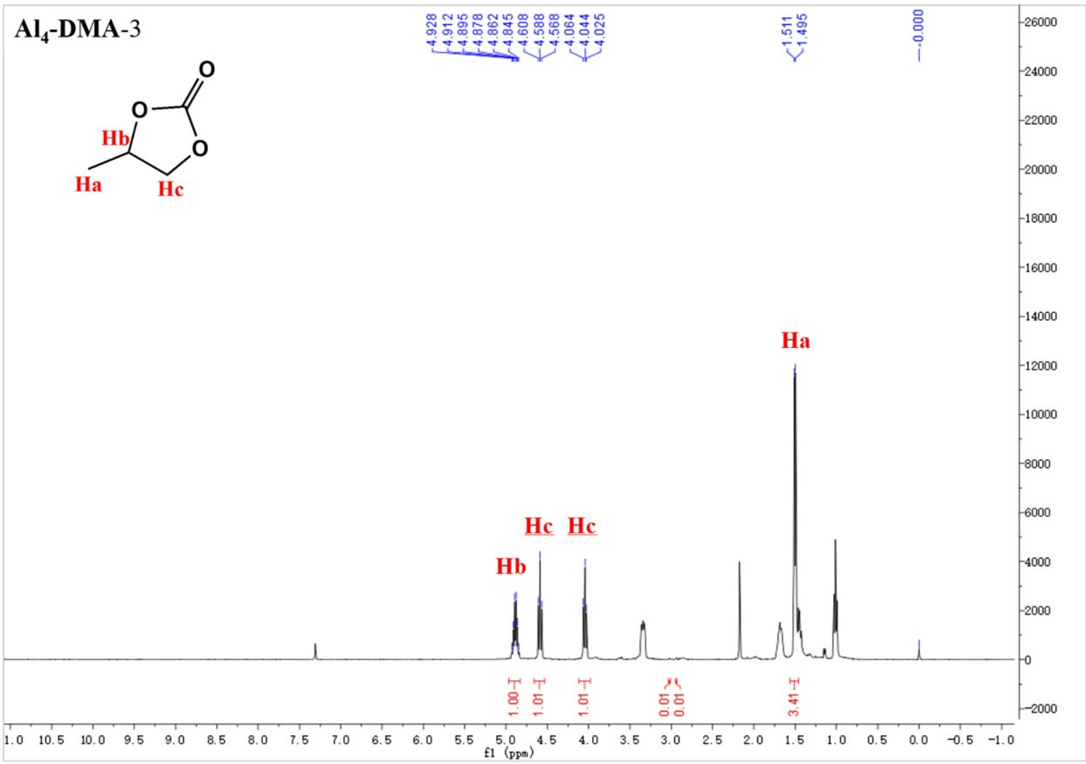

Fig. S13 ^{1}HNMR spectrum of **Al$_4$-DMA**-3 catalyzed oxidation products of ethylene oxide (400 MHz, $CDCl_3$, 298 K).

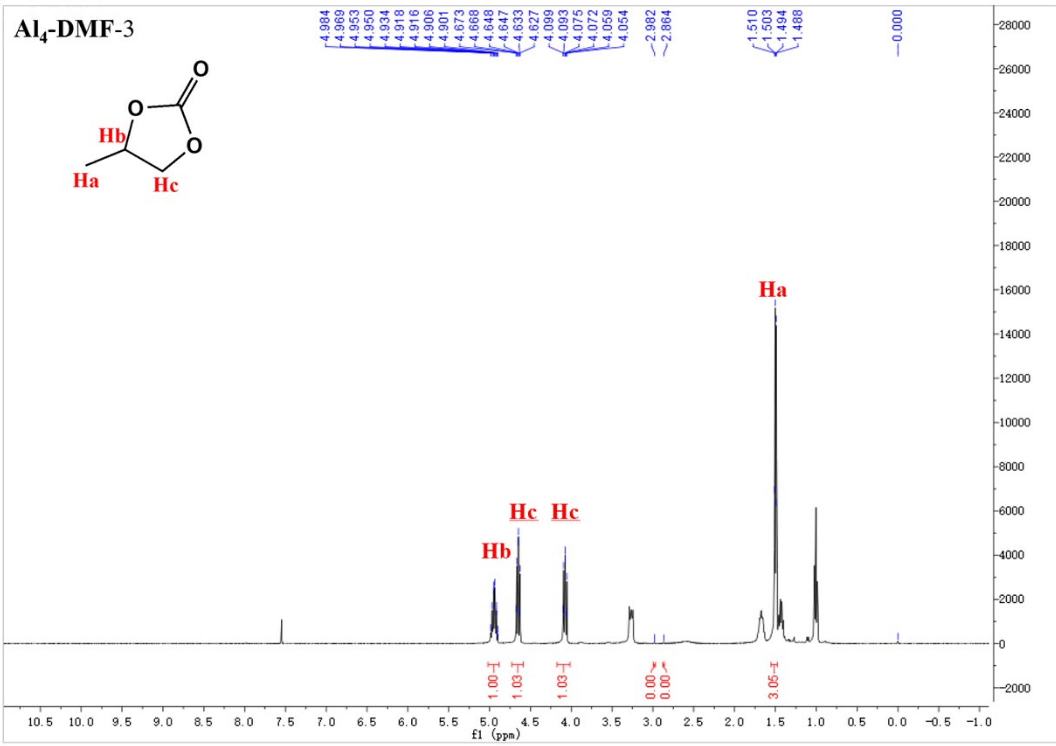

Fig. S14 [1]HNMR spectrum of **Al$_4$-DMF**-3 catalyzed oxidation products of ethylene oxide (400 MHz, $CDCl_3$, 298 K).

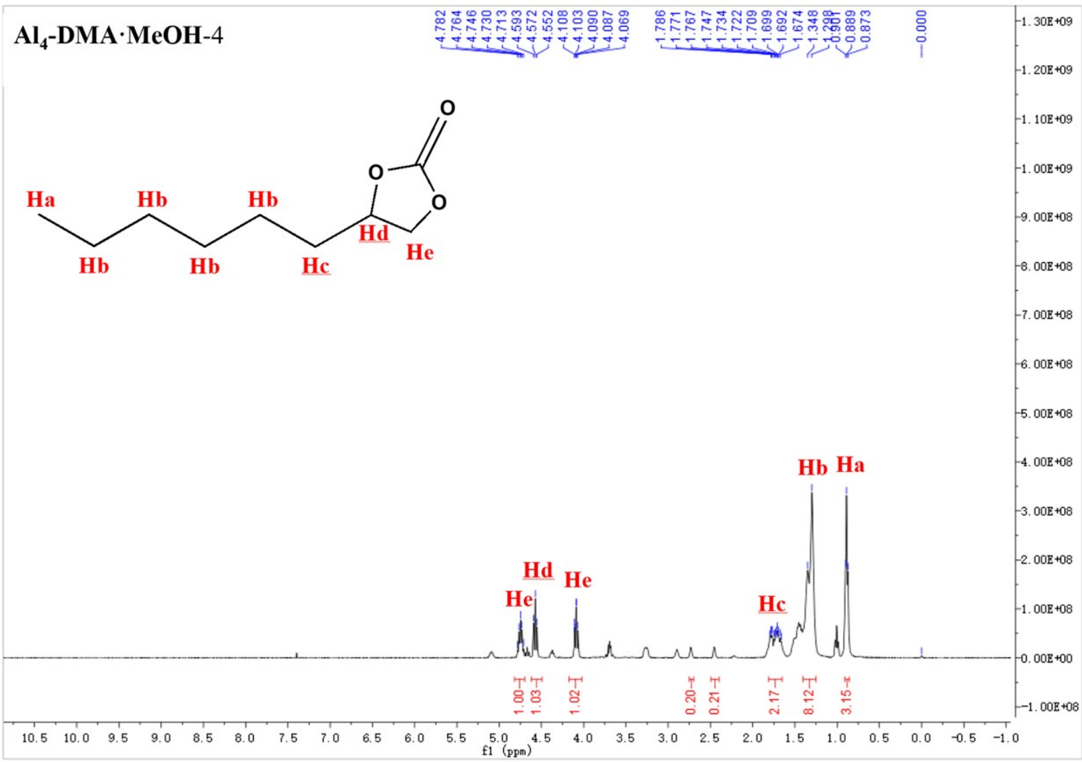

Fig. S15 [1]HNMR spectrum of **Al$_4$-DMA·MeOH**-4 catalyzed oxidation products of octane oxide (400 MHz, $CDCl_3$, 298 K).

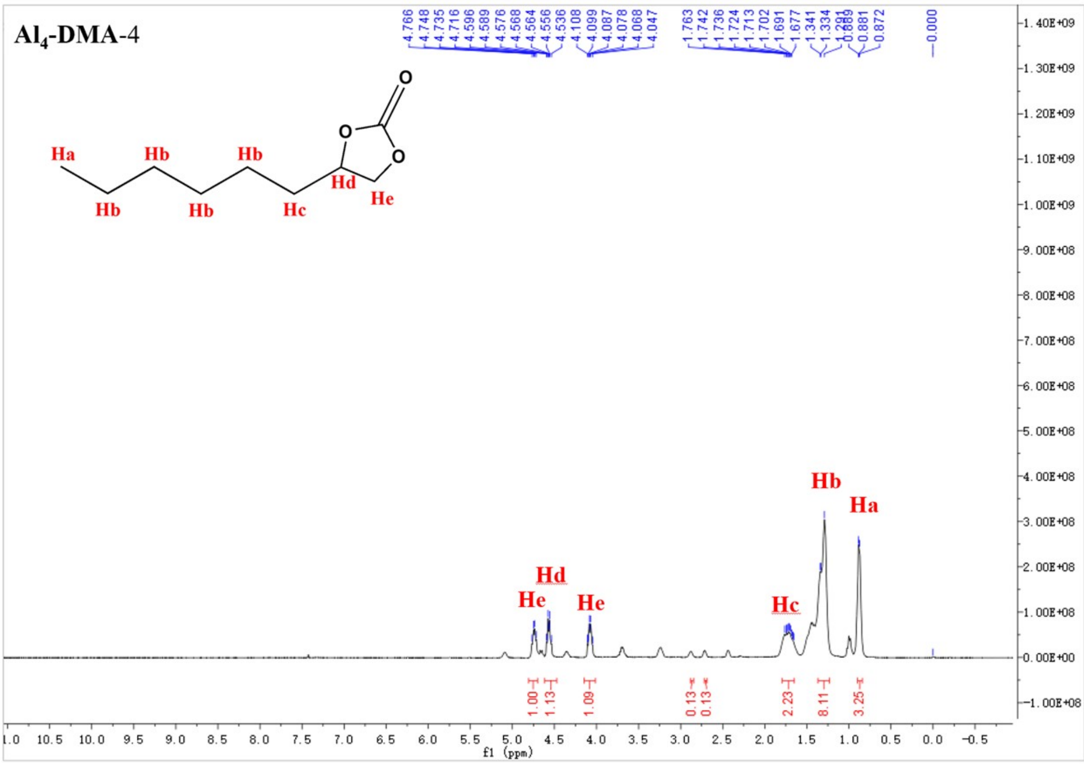

Fig. S16 [1]HNMR spectrum of **Al_4-DMA**-4 catalyzed oxidation products of octane oxide (400 MHz, $CDCl_3$, 298 K).

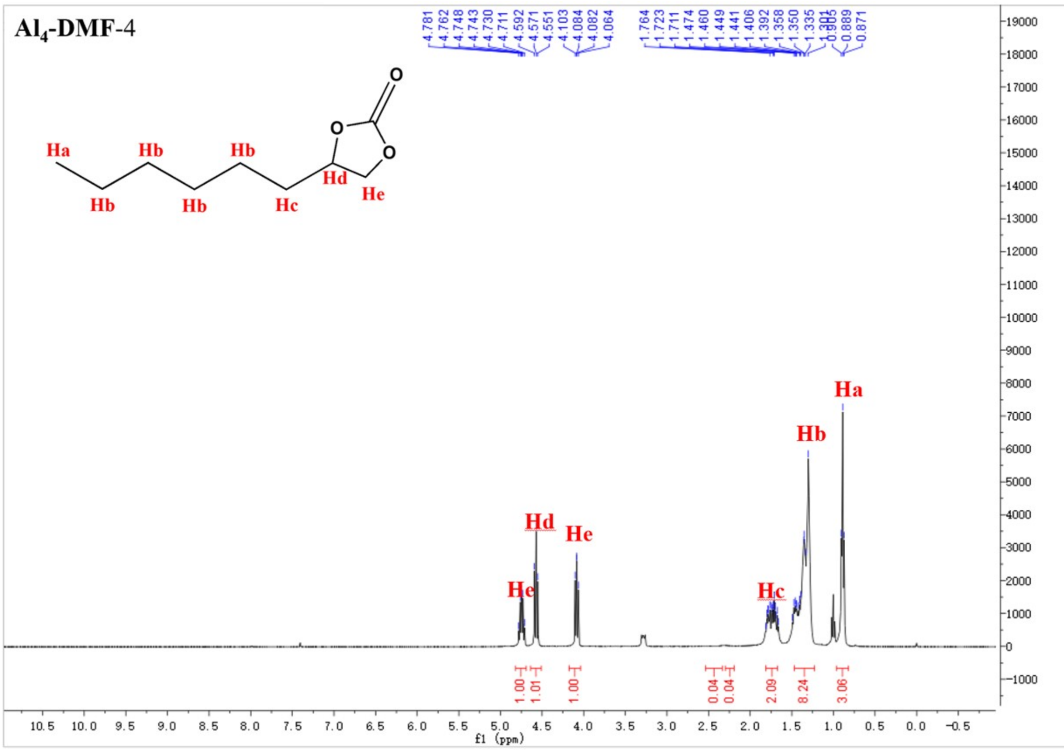

Fig. S17 [1]HNMR spectrum of **Al_4-DMF**-4 catalyzed oxidation products of octane oxide (400 MHz, $CDCl_3$, 298 K).

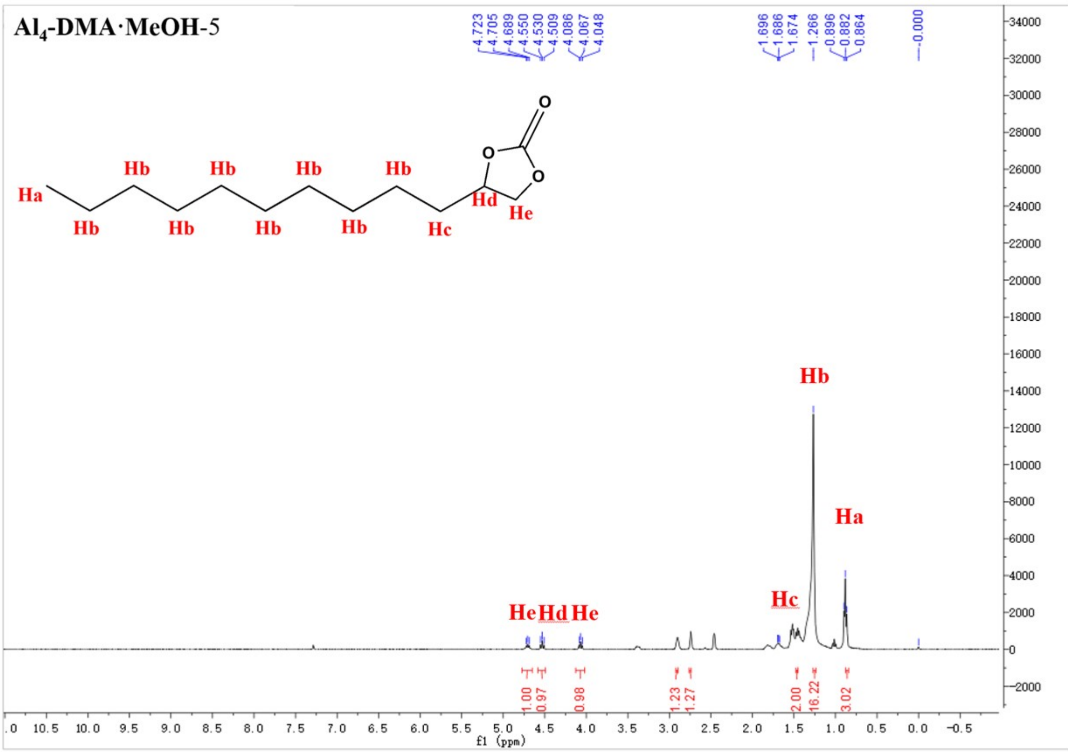

Fig. S18 [1]HNMR spectrum of **Al$_4$-DMA·MeOH**-5 catalyzed oxidation products of dodecane oxide (400 MHz, $CDCl_3$, 298 K).

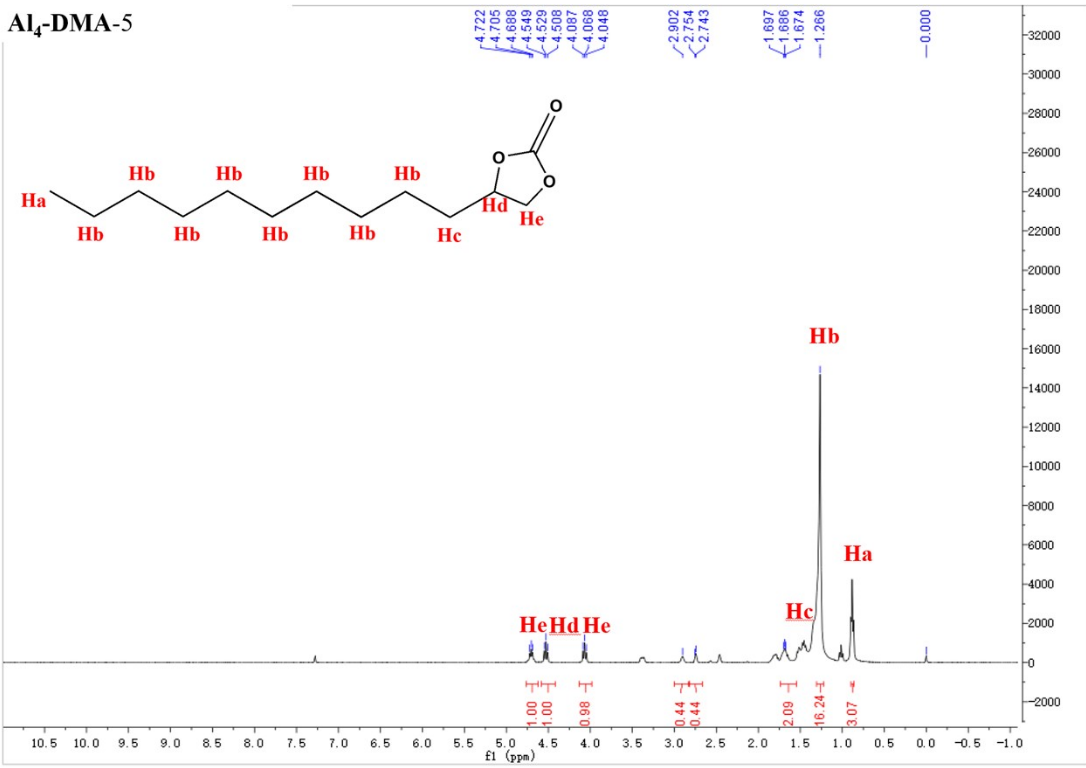

Fig. S19 [1]HNMR spectrum of **Al$_4$-DMA**-5 catalyzed oxidation products of dodecane oxide (400 MHz, $CDCl_3$, 298 K).

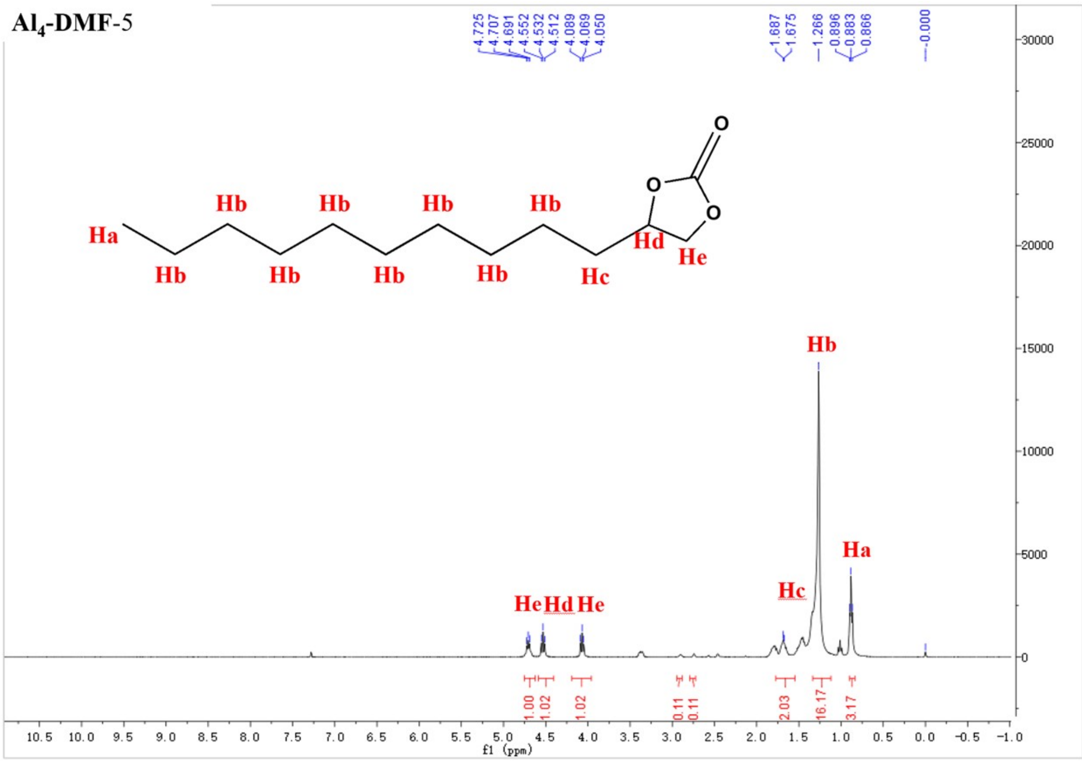

Fig. S20 [1]HNMR spectrum of **Al_4-DMF**-5 catalyzed oxidation products of dodecane oxide (400 MHz, $CDCl_3$, 298 K).

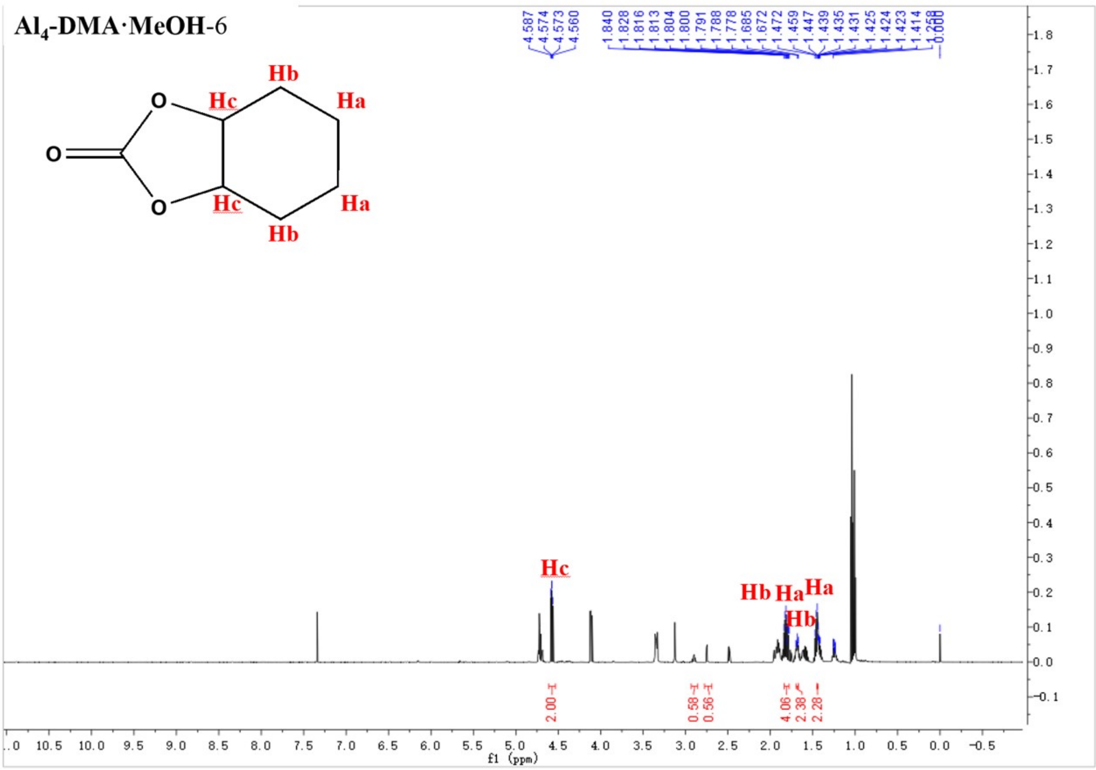

Fig. S21 [1]HNMR spectrum of **Al_4-DMA·MeOH**-6 catalyzed oxidation products of cyclohexane oxide (400 MHz, $CDCl_3$, 298 K).

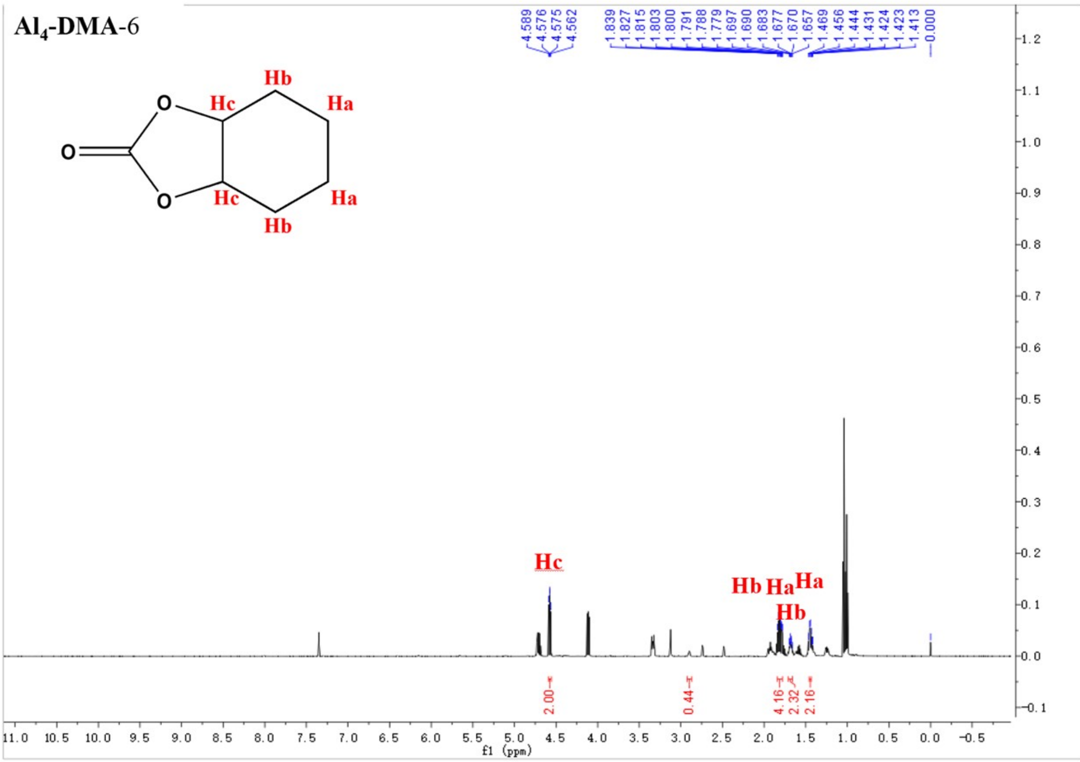

Fig. S22 [1]HNMR spectrum of **Al$_4$-DMA**-6 catalyzed oxidation products of cyclohexane oxide (400 MHz, $CDCl_3$, 298 K).

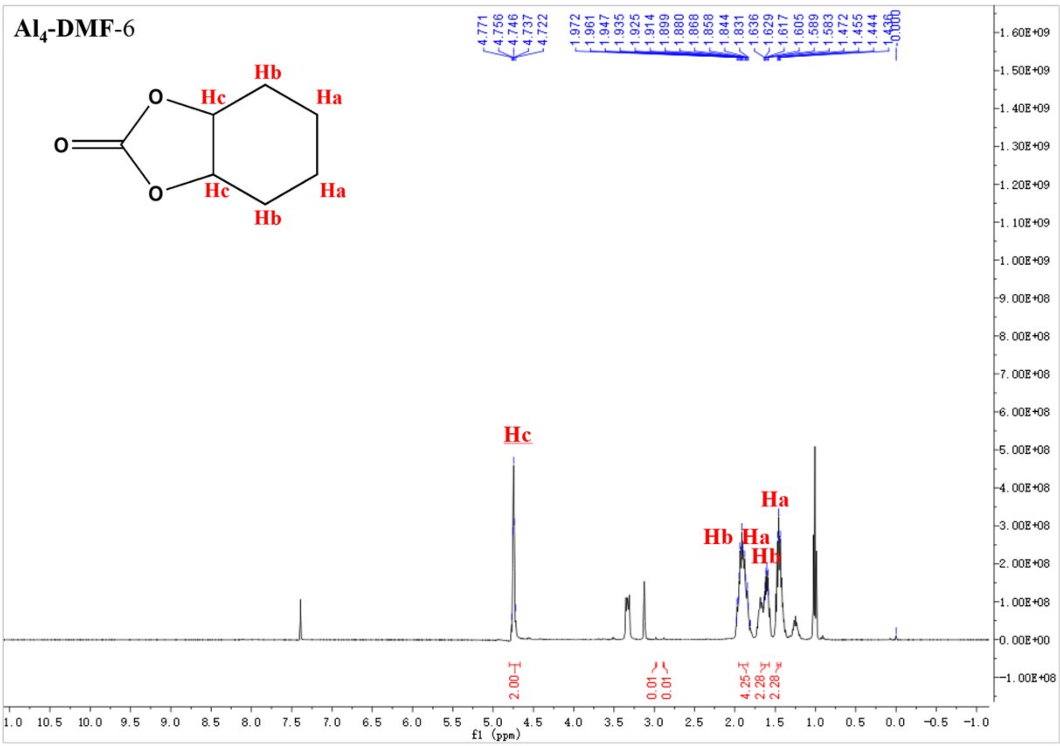

Fig. S23 [1]HNMR spectrum of **Al$_4$-DMF**-6 catalyzed oxidation products of cyclohexane oxide (400 MHz, $CDCl_3$, 298 K).

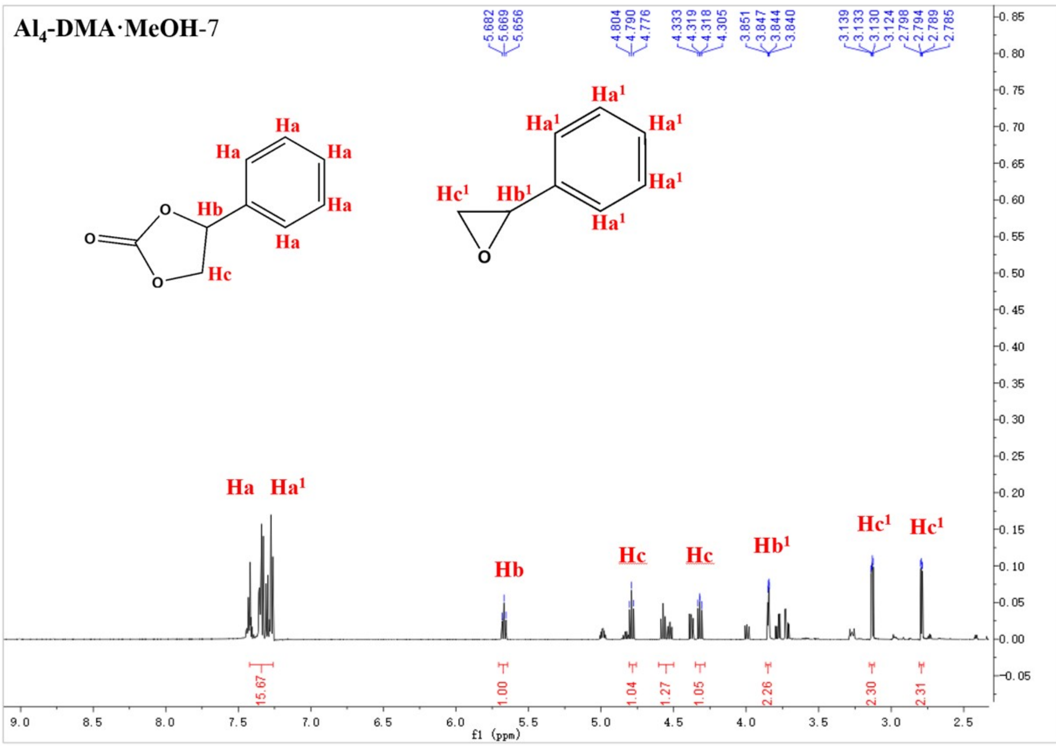

Fig. S24 [1]HNMR spectrum of **Al_4-DMA·MeOH-7** catalyzed oxidation products of (R)-styrene oxide (400 MHz, $CDCl_3$, 298 K).

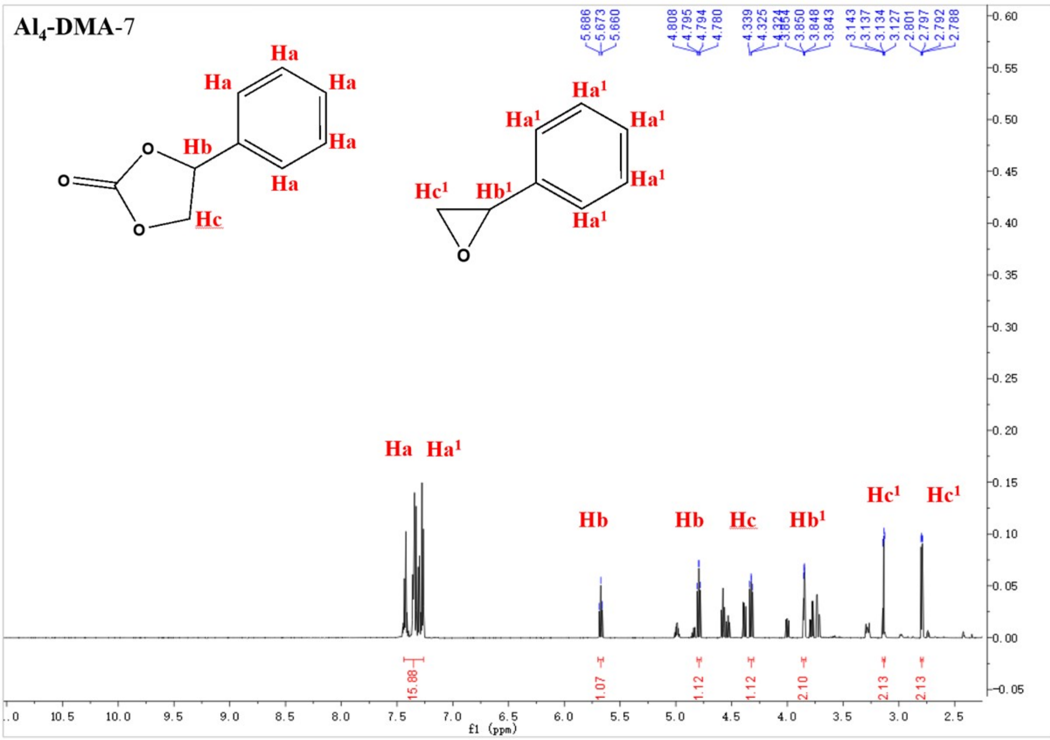

Fig. S25 [1]HNMR spectrum of **Al_4-DMA-7** catalyzed oxidation products of (R)-styrene oxide (400 MHz, $CDCl_3$, 298 K).

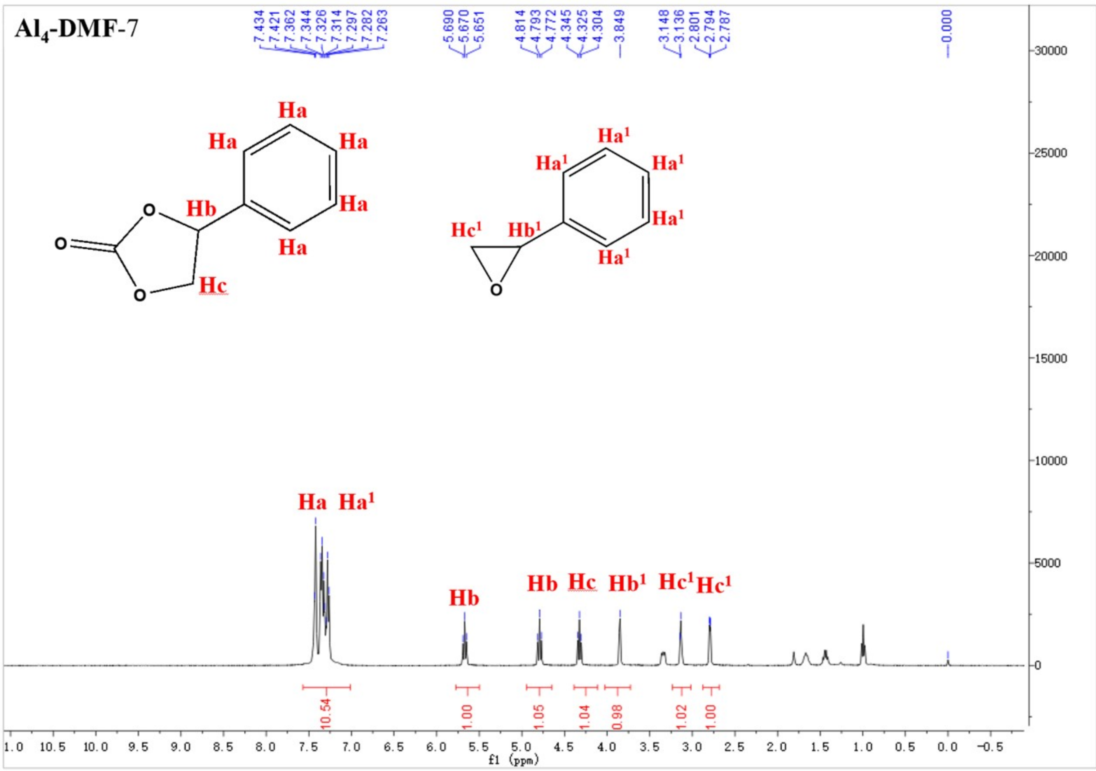

Fig. S26 [1]HNMR spectrum of **Al_4-DMF-7** catalyzed oxidation products of (R)-styrene oxide (400 MHz, $CDCl_3$, 298 K).

Table S4. Crystal data for **Al_4-DMA·MeOH**, **Al_4-DMA** and **Al_4-DMF.**

Identification code	**Al_4-DMA·MeOH**	**Al_4-DMA**	**Al_4-DMF**
Empirical formula	$C_{96}H_{122}Al_4N_2O_{32}S_8$	$C_{96}H_{128}Al_4N_4O_{32}S_8$	$C_{92}H_{120}Al_4N_4O_{32}S_8$
Formula weight	2132.31	2214.42	2158.31
Temperature/K	99.98(10)	100.00(10)	150.01(10)
Crystal system	monoclinic	monoclinic	triclinic
Space group	C_2/c	P_{21}/n	P-1
a/Å	23.4383(6)	15.3971(2)	12.04380(10)
b/Å	18.9600(2)	23.9137(2)	13.38600(10)
c/Å	27.5046(6)	17.5318(2)	19.3391(2)
α/°	90	90	95.7660(10)
β/°	118.351(3)	96.7090(10)	106.3040(10)
γ/°	90	90	107.2180(10)
Volume/Å^3	10756.7(5)	6411.03(12)	2800.45(5)
Z	4	2	1
ρ_{calc}g/cm^3	1.317	1.147	1.280
μ/mm^{-1}	2.494	2.114	2.407
F(000)	4496.0	2336.0	1136.0
Radiation	Cu Kα (λ = 1.54184)	Cu Kα (λ = 1.54184)	Cu Kα (λ = 1.54184)
$_2$Θ range for data collection/°	6.21 to 142.942	6.28 to 143.428	4.86 to 153.74
Index ranges	-27 ≤ h ≤ 28, -23 ≤ k ≤ 22,	-18≤ h ≤18, -29≤ k ≤29,	-15 ≤ h ≤ 15, -16 ≤ k ≤ 16,

	$-33 \leq l \leq 33$	$-21 \leq l \leq 21$	$-23 \leq l \leq 24$
Reflections collected	85620	108525	37965
Independent reflections	10059 [Rint = 0.1767, Rsigma = 0.0710]	12005 [Rint = 0.1183, Rsigma = 0.0448]	11333 [Rint = 0.0822, Rsigma = 0.0640]
Data/restraints/parameters	10059/68/641	12005/59/666	11333/6/647
Goodness-of-fit on F_2	1.205	1.042	1.103
Final R indexes [I>=$_2\sigma$ (I)]	R_1 = 0.1005, wR_2 = 0.2787	R_1 = 0.1025 wR_2 = $0_{.2682}$	R_1 = 0.0536, wR_2 = 0.1504
Final R indexes [all data]	R_1 = 0.1176, wR_2 = 0.3025	R_1 = 0.1178, wR_2 = 0.2838	R_1 = 0.0576, wR_2 = 0.1544
Largest diff. peak/hole / e $Å^{-3}$	2.09/-1.22	1.78/-0.83	0.62/-0.81

Table S5. Selected bond distances (Å) and angles (°) for **Al_4-DMA·MeOH**, **Al_4-DMA**, and **Al_4-DMF**.

Al_4-DMA·MeOH			
Al1—O1	1.836 (3)	O13—Al1—O11	178.36 (14)
Al1—O10	1.812 (3)	O13—Al1—O14	96.19 (14)
Al1—O11	2.125 (3)	O13—Al1—O14i	93.53 (13)
Al1—O13	1.849 (3)	O14i—Al1—O11	86.34 (12)
Al1—O14	1.850 (3)	O14—Al1—O11	85.37 (12)
Al1—O14i	1.870 (3)	O14—Al1—O14i	76.94 (12)
Al2—O4	1.815 (3)	O4—Al2—O5	87.50 (16)
Al2—O5	1.997 (3)	O4—Al2—O7	92.86 (16)
Al2—O7	1.854 (4)	O4—Al2—O15	173.27 (15)
Al2—O13	1.812 (3)	O4—Al2—O16	96.61 (18)
Al2—O15	1.977 (4)	O7—Al2—O5	88.94 (15)
Al2—O16	1.875 (4)	O7—Al2—O15	82.47 (16)
O1—Al1—O11	86.92 (13)	O7—Al2—O16	167.80 (18)
O1—Al1—O13	93.42 (13)	O13—Al2—O4	95.30 (14)
O1—Al1—O14	95.17 (12)	O13—Al2—O5	174.41 (16)
O1—Al1—O14i	170.01 (13)	O13—Al2—O7	95.73 (14)
O10—Al1—O1	94.39 (13)	O13—Al2—O15	90.01 (14)
O10—Al1—O11	86.50 (12)	O13—Al2—O16	91.05 (15)
O10—Al1—O13	91.87 (13)	O15—Al2—O5	87.57 (16)
O10—Al1—O14	167.08 (14)	O16—Al2—O5	83.81 (17)
O10—Al1—O14i	92.55 (12)	O16—Al2—O15	87.41 (18)
Symmetry code: (i) −*x*+1/2, −*y*+3/2, −*z*+1.			
Al_4-DMA			
Al1—O1	1.866 (4)	O14—Al1—O5	175.1 (2)
Al1—O2	1.845 (4)	O14—Al1—O15	92.02 (17)
Al1—O5	2.039 (4)	O14—Al1—O16	99.17 (19)
Al1—O14	1.821 (3)	O15—Al1—O5	86.09 (16)
Al1—O15	1.878 (4)	O15—Al1—O16	84.4 (2)
Al1—O16	1.900 (5)	O16—Al1—O5	85.19 (18)
Al2—Al2i	2.896 (3)	O3—Al2—O9	86.44 (13)
Al2—O3	1.861 (3)	O3—Al2—O13	90.16 (18)
Al2—O4	1.810 (5)	O4—Al2—O3	93.54 (17)
Al2—O9	2.234 (3)	O4—Al2—O9	80.37 (17)
Al2—O13i	1.860 (4)	O4—Al2—O13i	96.01 (17)
Al2—O13	1.863 (4)	O4—Al2—O13	167.12 (16)
Al2—O14	1.835 (3)	O4—Al2—O14	95.7 (2)
O1—Al1—O5	88.98 (16)	O13i—Al2—O3	164.12 (19)

O1—Al1—O15	170.8 (2)	O13—Al2—O9	87.57 (17)
O1—Al1—O16	87.5 (2)	O13i—Al2—O9	82.69 (13)
O2—Al1—O1	94.22 (16)	O13i—Al2—O13	77.88 (18)
O2—Al1—O5	84.26 (17)	O14—Al2—O3	98.09 (14)
O2—Al1—O15	93.05 (19)	O14—Al2—O9	174.2 (2)
O2—Al1—O16	169.29 (16)	O14—Al2—O13	96.00 (19)
O14—Al1—O1	93.50 (16)	O14—Al2—O13i	93.56 (15)
O14—Al1—O2	91.30 (18)		
Symmetry code: (i) −*x*+1, −*y*+1, −*z*.			
Al_4-DMF			
Al1—O8	2.0829 (14)	O11—Al1—O8	86.97 (6)
Al1—O11	1.8367 (15)	O11—Al1—O12	91.87 (7)
Al1—O12	1.8437 (15)	O11—Al1—O14i	169.93 (7)
Al1—O13	1.8338 (14)	O11—Al1—O16	84.65 (7)
Al1—O14i	1.8744 (15)	O12—Al1—O8	87.44 (6)
Al1—O16	1.9169 (16)	O12—Al1—O14i	91.26 (7)
Al2—O4	2.0466 (15)	O12—Al1—O16	171.59 (7)
Al2—O9	1.8383 (15)	O13—Al1—O8	177.14 (6)
Al2—O10	1.8660 (15)	O13—Al1—O11	93.30 (6)
Al2—O13	1.8440 (15)	O13—Al1—O12	95.39 (6)
Al2—O14	1.8801 (15)	O13—Al1—O14i	95.93 (6)
Al2—O15	1.9210 (15)	O13—Al1—O16	92.46 (6)
O14—Al2—O4	85.95 (6)	O14i—Al1—O8	83.61 (6)
O14—Al2—O15	87.08 (7)	O14i—Al1—O16	90.92 (7)
O15—Al2—O4	85.07 (6)	O16—Al1—O8	84.73 (6)
O13—Al2—O10	92.16 (6)	O9—Al2—O4	87.37 (6)
O13—Al2—O14	95.13 (6)	O9—Al2—O10	93.25 (7)
O13—Al2—O15	93.48 (7)	O9—Al2—O13	94.12 (6)
O10—Al2—O14	171.74 (7)	O9—Al2—O14	90.10 (7)
O10—Al2—O15	88.61 (7)	O9—Al2—O15	172.10 (7)
O13—Al2—O4	178.15 (7)	O10—Al2—O4	86.67 (6)
Symmetry code: (i) −x+1, −*y*+1, −*z*+1.			